Author Manuscript
Author Manuscript
Author Manuscript
Author Manuscript

HHS Public Access
Author manuscript
Bone. Author manuscript; available in PMC 2019 September 16.

Published in final edited form as:
Bone. 2017 April ; 97: 153–167. doi:10.1016/j.bone.2017.01.022.

Inhibition of Osteoclast Differentiation and Collagen Antibody-Induced Arthritis by CTHRC1

Yong-Ri Jin[1], **J. Patrizia Stohn**[1], **Qiaozeng Wang**[1], **Kenichi Nagano**[2], **Roland Baron**[2], **Mary L. Bouxsein**[3], **Clifford J. Rosen**[1], **Vyacheslav A. Adarichev**[4], **Volkhard Lindner**[1]

[1]Center for Molecular Medicine, Maine Medical Center Research Institute, Scarborough, ME

[2]Department of Oral Medicine, Infection and Immunity, Harvard School of Dental Medicine, Boston, MA

[3]Harvard Medical School, Beth Israel Deaconess Medical Center, Boston, MA

[4]Department of Biology, Nazarbayev University, Astana, Kazakhstan

Abstract

Collagen triple helix repeat-containing1 (*Cthrc1*) has previously been implicated in osteogenic differentiation and positive regulation of bone mass, however, the underlying mechanisms remain unclear. Here we characterized the bone phenotype of a novel *Cthrc1* null mouse strain using bone histomorphometry, μCT analysis and functional readouts for bone strength. In male *Cthrc1* null mice both trabecular bone as well as cortical bone formation was impaired, whereas in female *Cthrc1* null mice only trabecular bone parameters were altered. Novel and highly specific monoclonal antibodies revealed that CTHRC1 is expressed by osteocytes and osteoblasts, but not osteoclasts. Furthermore, *Cthrc1* null mice exhibited increased bone resorption with increased number of osteoclast and increased osteoclast activity together with enhanced expression of osteoclastogenic genes such as *c-Fos*, *Rankl*, *Trap*, and *Nfatc1*. Differentiation of bone marrow-derived monocytes isolated from *Cthrc1* null mice differentiated into osteoclasts as effectively as those from wildtype mice. In the presence of CTHRC1 osteoclastogenic differentiation of bone marrow-derived monocytes was dramatically inhibited as was functional bone resorption by osteoclasts. This process was accompanied by downregulation of osteoclastogenic marker genes, indicating that extrinsically derived CTHRC1 is required for such activity. *In vitro*, CTHRC1 had no effect on osteogenic differentiation of bone marrow stromal cells, however, calvarial osteoblasts from *Cthrc1* null mice exhibited reduced osteogenic differentiation compared to osteoblasts from wildtypes. In a collagen antibody-induced arthritis model *Cthrc1* null mice suffered significantly more severe inflammation and joint destruction than wildtypes, suggesting that CTHRC1 expressed by the activated synoviocytes has anti-inflammatory effects. Mechanistically, we found that CTHRC1 inhibited NFκB activation by preventing IκBα degradation while also inhibiting ERK1/2 activation. Collectively our studies demonstrate that CTHRC1 secreted from osteocytes and osteoblasts functions as an inhibitor of osteoclast differentiation via inhibition of NFκB-dependent signaling. Furthermore, our data suggest that CTHRC1 has potent anti-inflammatory properties that limit arthritic joint destruction.

Corresponding author: Volkhard Lindner, M.D., Ph.D., Maine Medical Center Research Institute, 81 Research Drive, Scarborough, ME 04074, Phone: 207-396-8143, Fax: 207-396-8179, lindnv@mmc.org.

Author Manuscript Author Manuscript Author Manuscript Author Manuscript

Keywords

osteoclastogenesis; arthritis; bone strength; CTHRC1; NFκB

1. Introduction

We originally discovered collagen triple helix repeat containing 1 (*Cthrc1*) in a screen for novel sequences induced in injured arteries, where we found *Cthrc1* expressed in adventitial cells of remodeling arteries but not in uninjured vessels (1). Our subsequent studies also demonstrated that CTHRC1 is characteristically expressed by the activated fibroblast associated with wound healing as well as cancer-activated fibroblast (2,3). Kimura et al. (4) first reported that *Cthrc1* null mice exhibit reduced bone mass, and *in vitro* osteogenic differentiation of bone marrow stromal cells revealed that endogenously expressed Cthrc1 is required for effective osteogenic differentiation by affecting cell proliferation and differentiation (4). In contrast, it was recently reported that CTHRC1 stimulates bone formation *in vitro* and that it functions as a coupling factor *in vivo*, produced by mature actively resorbing osteoclasts. The key difference between the two studies is the identity of the CTHRC1-producing cell, which in the absence of specific and reliable antibody reagents has remained controversial.

To understand the in vivo function of CTHRC1 during adulthood, we recently generated a targeted *Cthrc1* null allele by replacing exon 2, 3 and 4 with a neomycin cassette (3). We reported that on the C57BL/6J background, our *Cthrc1* null mice develop fatty livers with extensive macrovesicular steatosis (5). Using highly specific monoclonal antibodies we found that CTHRC1 is prominently expressed by neuroendocrine cells of the hypothalamus (5), which are likely sources contributing to circulating levels of CTHRC1 detectable in plasma (2). We also identified bone as another tissue that constitutively expresses CTHRC1 in the adult (3). The recent study by Takeshita et al (6) reported that deletion of floxed *Cthrc1* alleles with a *cathepsin-K-Cre* strain (*Ctsk*) could fully recapitulate the bone phenotype observed in global knockout mice, whereas an osteoblast lineage specific knockout of *Cthrc1* did not recapitulate the bone phenotype. A recent study, however, demonstrated that *Ctsk* is also expressed in mesenchymal progenitor cells, indicating *Ctsk-Cre* mediated *Cthrc1* deletion will not be restricted to osteoclasts (7).

To eliminate potential effects of circulating CTHRC1 on bone formation the present study investigated the functions of CTHRC1 in bone using a global *Cthrc1* null mutant mouse on a pure C57BL/6J background. In addition, analyses were performed on both males and females. Using primary cultures of bone marrow stromal cells and calvarial osteoblasts for osteogenic differentiation, and bone marrow-derived monocytes together with RAW264.7 cells for osteoclastogenic differentiation we elucidated the mechanism of CTHRC1 function in bone homeostasis.

Author Manuscript Author Manuscript Author Manuscript Author Manuscript

2. Materials and Methods

2.1. Reagents and antibodies

Penicillin, streptomycin, and α-minimum essential medium (α-MEM) were obtained from Mediatech (Herndon, VA), and fetal bovine serum (FBS) was obtained from Atlanta Biologicals. Soluble, recombinant murine M-CSF and human recombinant RANKL were obtained from PeproTech (Rocky Hill, NJ) and R&D Systems (Minneapolis, MN). Anti-phospho-ERK1/2, anti-IκBα, anti-phospho-IκBα, anti-phospho-p65 (p-NFκB) and anti-cleaved caspase-3 antibodies were from Cell Signaling Technology, Inc. (Beverly, MA). Anti-mouse and anti-rabbit HRP conjugated IgGs were purchased from Jackson ImmunoResearch Laboratories, Inc (West Grove, PA). Tartrate-resistant acid phosphatase (TRAP) immunostaining was performed with biotinylated monoclonal anti-TRAP (1:500, clone ACP5/1070, Novus Biologicals). Apoptosis of calvarial osteoblasts derived from *Cthrc1* null and wildtype mice was assessed by immunocytochemistry for activated caspase-3. Rabbit and mouse monoclonal anti-CTHRC1 antibodies were previously characterized and described (www.mmcri.org/antibody) (2).

Rabbit monoclonal anti-Cthrc1 clone Vli-55 (www.mmcri.org/antibody) was used for Western blotting and immunohistochemistry on paraffin-embedded, formalin-fixed tissues as described (3). For Western blotting of mouse tissue lysates for CTHRC1, the Avidin/Biotin Blocking Kit (Vector, Burlingame, CA) was used, followed by incubation with biotinylated Vli-08G09 (10ng/mL) using the EZ-Link Biotinylation Kit (LC spacer) from Thermo Scientific (Rockford, IL), followed by incubation with Streptavidin-HRP (Vector, Burlingame, CA).

Unmodified human CTHRC1 (hCTHRC1) was produced in CHO-K1 cells by adenovirus transduction as described (3). Prior evidence (not shown) suggested that C-terminally tagged CTHRC1 may interfere with function and therefore only wildtype hCTHRC1 was used in the form of serum-free conditioned medium (hCTHRC1-CM) added to the culture medium (60% final). All hCTHRC1-CM used was tested for hCTHRC1 concentration by ELISA (2) with hCTHRC1 levels consistently in the 100 ng/mL range. Serum-free conditioned medium from CHO-K1 cells transduced with a beta-galactosidase expressing adenovirus was used as a control. For experiments using hCTHRC1-depleted hCTHRC1-CM, the conditioned medium was incubated with monoclonal anti-hCTHRC1 IgGs Vli-13E09 and Vli-10G07 (1 μg/mL each, 3 hours at 4°C), followed by removal of the hCTHRC1/antibody complexes with Protein A Sepharose (CL-4B, Amersham) chromatography.

2.2. Mice

All protocols involving animals were approved by the Institutional Animal Care and Use Committee of the Maine Medical Center (protocol number 1505) and were in compliance with all applicable regulations and guidelines including the National Institutes of Health *Guide for Care and Use of Laboratory Animals*. *Cthrc1* null mice were derived from matings of homozygous Cthrc1^{tm1Vli} mutants on the C57BL/6J background as described previously (3). C57BL/6J wildtype mice were used as controls. Mice were fed a standard rodent diet (Harlan, 2018 Teklad Global 18% Protein Rodent Diet) and water ad libitum, and housed

Author Manuscript Author Manuscript Author Manuscript Author Manuscript

with dry cellulose bedding (Harlan, 7070 Diamond) under a 14-hour daylight-10 hour night cycle.

2.3. Bone analyses

To evaluate bone volume and architecture by micro-computed tomography (μCT), mouse tibiae were fixed in 70% ethanol and scanned using a Scanco μCT instrument (Scanco Medical) at several resolutions for both overall tibial assessment and structural analysis of trabecular and cortical bone. Trabecular bone parameters were calculated using the Scanco software to analyze the bone scans from the trabecular region directly distal to the proximal tibial growth plate. Bone histomorphometric analyses were conducted in the Baron laboratory on non-decalcified sections as previously described (8,9). Calcein (Sigma/Aldrich, 20 mg/kg injected 7 days before euthanasia) and demeclocycline (Sigma/Aldrich, 30 mg/kg injected 2 days before euthanasia) were used to label bone. Terminology and units follow the recommendations of the Histomorphometry Nomenclature Committee of the American Society for Bone and Mineral Research (10,11).

2.4. Mechanical testing

Femurs were mechanically tested in three-point bending using an electromechanical materials testing machine (Synergie 100, MTS Systems, Eden Prairie, MN) as described (12).

2.5. Western blotting

Western blotting of bone and marrow tissue lysates was performed as previously described using primary antibodies (anti-Cthrc1, 10 ng/ml; anti-actin, 1:1000) followed by secondary antibodies (1:5000) conjugated with horseradish peroxidase (HRP) (2). Marrow was separated from bone by blowing it out of the shaft with a pipet.

Quantitative evaluation of immunoblots was performed by densitometry using ImageJ software.

2.6. DNA transfection and luciferase reporter assays

An expression vector for constitutively active IKKβ (Addgene, IKK-2 S177E S181E) or pcDNA3.0 was used to transfect RAW264.7 cells with Fugene 6 (Roche) transfection reagent in OPTM-1 medium, which was replaced with osteoclastogenic differentiation medium 24 hours later. For the reporter assays, the Dual-Luciferase Reporter Assay (Promega) was used with RAW264.7 cells cotransfected with luciferase reporter plasmids (NFκB-Luc and AP1-Luc, PathDetect, Agilent Technologies). 24 hours later the cells were stimulated with differentiation medium containing RANKL (100 ng/mL) in the presence of control-CM or hCTRHC1-CM before harvesting cell lysates for analyses 24 hours later. All assays were performed in replicates of ≥3.

2.7. Quantitative RT-PCR

The methods for this were previously described (5). All primer sequences are listed in the Supplemental data Table 1.

Author Manuscript Author Manuscript Author Manuscript Author Manuscript

2.8. Osteoclastogenic differentiation

Osteoclasts were differentiated from mouse bone marrow monocytes as described elsewhere (13). Briefly, bone marrow cells were purified with a 40 μm cell strainer to remove mesenchymal cells, cultured with 40 ng/mL of M-CSF in α-MEM containing 10% FBS for 3 days until cells reached confluence. Then the cells were differentiated for 9 days with M-CSF (40 ng/mL) and RANKL (100 ng/mL) in the presence of serum-free conditioned medium harvested from control transfected CHO-K1 cells (Control-CM), CHO-K1 cells stably transfected with a beta-galactosidase- (Control-CM) or hCTHRC1 adenovirus transduced CHO-K1 cells (hCTHRC1-CM) and 10% FBS. At day 9, the culture was terminated, and cells were then fixed with 2.5% glutaraldehyde (Sigma). Osteoclasts were identified by tartrate-resistant acid phosphatase staining kit (Sigma/Aldrich). Mature osteoclasts were identified as multinucleated (>3 nuclei) $TRAP^+$ cells.

RAW264.7 cells were cultured in α-MEM containing 10% FBS. Osteoclastogenic differentiation was induced by addition of RANKL (100 ng/mL) to the culture medium. Differentiation was allowed to continue for 4–5 days with media changed every 2 days.

2.9. Osteoblastic cell culture and assays

Osteoblasts were differentiated from mouse bone marrow stromal cells and calvarial osteoblasts as described (13). To culture osteoblasts, bone marrow was harvested from femurs and tibiae of wildtype and *Cthrc1* null mice (n=3). Bone marrow cells were dispersed by passage through a 25G needle 5 times. Cells were plated in 12-well plates ($5x10^6$ cells/well) in plating medium (α-MEM containing 10% FBS) and cultured for 3 days before cells reached confluence. Primary calvarial osteoblasts were isolated from newborn calvaria by sequential digestion with 0.42 mg/mL collagenase P (Roche) and trypsin (0.5%, Gibco). Primary osteoblastic cells from the second to fourth fraction were pooled and used for osteogenic differentiation. To induce osteogenic differentiation, α-MEM containing 10% FBS, β-glycerophosphate (8 mM) and ascorbic acid (50 μg/mL) was used and the medium was replaced every other day over a 21 day period. Early osteogenic differentiation was assessed by alkaline phosphatase histochemistry (86R-1KT, Sigma-Aldrich), whereas mature bone formation was determined by Alizarin red staining and von Kossa staining as described.

2.10. Colony-forming assay

To determine potential effects of CTHRC1 on bone marrow stromal cells and bone marrow derived monocyte proliferation, we performed colony-forming assays by seeding 0.5×10^6 cells/mL from *Cthrc1* null mice in 6 well tissue culture plates in growth medium as described above, supplemented with either control LacZ conditioned-medium or CTHRC1 conditioned-medium. After four days of culture, the culture medium was removed and the cells were fixed with 4% paraformaldehyde for 10 min, and cell colonies were stained using crystal violet.

2.11. Bone resorption assay

Bone resorption was assessed by culturing bone marrow cells in Osteo Assay Surface 96-well plates (Corning Life Sciences, Lowell, MA, USA) as previously described (14). In

Author Manuscript Author Manuscript Author Manuscript Author Manuscript

brief, bone marrow monocytes isolated from *Cthrc1* null mice were cultured with differentiation medium containing control LacZ conditioned-medium or CTHRC1 conditioned-medium as described above. Differentiation media was changed every 3 days until the end of a 17-day culture period. After wells were washed with PBS, 150 μL of 10% sodium hypochlorite was added to each well and incubated for 5 min. Wells were washed twice with water, and stained with a modified von Kossa stain (5%[w/v] aqueous silver nitrate solution) in the dark for 30 min. After staining, wells were soaked in water for 5min, and treated with 100 μL of 5% sodium carbonate (w/v in 10% formalin). Incubating for 5 min at room temperature reduces ionic silver to metallic silver, and the unresorbed mineralized surface turns black, whereas the resorbed areas are white. Digital images were captured and the percentage of resorbed area/well was quantified using ImageJ software. Eight wells were assessed per treatment.

2.12. Collagen antibody-induced arthritis model

Female homozygous Cthrc1^{tm1Vli} mutants on the C57BL/6J background and wildtype C57BL/6J controls (n=4 per group, 10–12 weeks of age) were injected intraperitoneally with the anti-collagen II antibody cocktail (Chondrex Inc., catalog # 53010, 5 mg/mouse). Two days later all mice received an intraperitoneal injection of lipopolysaccharide (Chondrex Inc., catalog # 9028, 50 μg/mouse). Arthritis was scored in a blinded fashion on days 7, 10, 14, and 21 after the antibody injection. Score 0: normal; score 1: mild but definite redness and swelling of the ankle or front paw, or apparent redness and swelling limited to individual digits, regardless of the number of affected digits; score 2: moderate redness and swelling of ankle or front paw; score 3: severe redness and swelling of the entire paw including digits; score 4: maximally inflamed limb with involvement of multiple joints. Mice were euthanized 21 days after the antibody injection for analysis of bones by histology. Histology scoring of arthritis combined for ankle and knee joints was performed in a blinded manner by scoring the amount/area of inflammatory cells on a scale from 0 (no) to 4 (maximal) inflammation. Bone erosion and pannus infiltrating the calcaneus was quantified by image analysis measuring the area of eroded bone and pannus surrounding the cortical bone of the calcaneus. The Mann-Whitney U test (GraphPad Prism) was used to assess statistical significance.

2.13. Statistical analyses

Statistical analyses were performed in GraphPad Prism (Version 5, GraphPad Software, Inc., San Diego, CA). Means of data for *Cthrc1* null mice and wildtype mice were compared using Student's t-test. Values for $p<0.05$ were considered statistically significant. With the expected differences between groups we calculated that a sample size of 6 in each group (unless stated otherwise) would have 80% power (p=0.05) to detect a significant difference in means for the bone parameters. In the collagen antibody-induced arthritis model 80% power was achieved with n=4 mice per group.

Author Manuscript Author Manuscript Author Manuscript Author Manuscript

3. Results

3.1. CTHRC1 is expressed in bone-forming cells

To determine where CTHRC1 is expressed in bone we performed immunohistochemistry, Western blotting and RT-PCR to identify the cell types and compartments of femurs that express CTHRC1. Immunoreactive CTHRC1 localized specifically to osteoblasts lining bone surfaces, whereas adjacent multinucleated osteoclasts did not express CTHRC1 (Fig. 1A). TRAP expression characteristic for osteoclasts revealed no overlap with expression of CTHRC1 as analyzed by confocal microscopy of double immunolabeling (Fig. 1B). CTHRC1 was also expressed by some but not all osteocytes where it localized to osteocyte processes of individual cells (Fig. 1C–E. arrows). CTHRC1 immunoreactivity within the osteocyte canaliculi is suggestive of CTHRC1 secretion into the extracellular space (Fig. 1C–F). Complete absence of any staining performed on femur sections from *Cthrc1* null mice confirmed specificity of the immunostaining performed with the monoclonal antibody (Fig. 1G). RT-PCR and Western blotting were used to confirm the immunohistochemistry results. RNA isolated from bone marrow, cortical bone (midshaft) and trabecular bone (proximal and distal epiphysis) showed expression of the *Cthrc1* transcript in the bone fractions but not the marrow (Fig. 1H). We also determined *Cthrc1* expression during osteogenic differentiation of bone marrow stromal cells (BMSCs) and found that these cells express *Cthrc1* with transcript levels increasing as cells differentiate (Fig. 1I). Western blot analysis of lysates prepared separately from the bone and marrow fraction further confirmed the absence of CTHRC1 in marrow cells (Fig. 1J). The biotinylated monoclonal antibody showed no CTHRC1 band in samples from *Cthrc1* null mice (Fig. 1G). These results indicate that CTHRC1 in bone is derived from osteoblasts and osteocytes but not osteoclasts.

3.2. Bone formation is altered in *Cthrc1* null mice

Previous studies indicated that CTHRC1 affects bone formation (4,6). Unlike previous studies our *Cthrc1* null mice analyzed here were on a pure C57BL/6J genetic background. Our targeting strategy generated a global null mutant that eliminated the potential confounding effects of circulating CTHRC1 expressed in tissues other than bone (2,3). In addition, we analyzed bones from males and females. The skeletal phenotype of 8 week old *Cthrc1* knockout mice was analyzed by histology, histomorphometry and μCT performed on non-decalcified specimens. As shown in Table 1 and Fig. 2, *Cthrc1*$^{\mathrm{tm1}\,Vli}$ mice clearly show lower trabecular bone mass compared to wildtypes in both genders. All the structure parameters [Bone Volume (BV/TV), Trabecular Thickness (Tb.Th), Trabecular Number (Tb.N) and Trabecular Separation (Tb.Sp)] in female *Cthrc1* null mice showed significant differences, and the same trends occurred in male mice, even though changes in some parameters did not reach significance. To understand the mechanism that led to lower trabecular bone mass in these *Cthrc1*$^{\mathrm{tm1}\,Vli}$ mice, we assessed the dynamic and cellular parameters of bone remodeling. The dynamic parameters of bone formation [MAR (Mineral Apposition Rate), Bone Formation Rate (BFR)] showed significant decreases in *Cthrc1* null mice compared to wildtypes (for example, BFR/BS was decreased almost 30% in male and 45% in female). It is important to note here that most of the decrease in bone formation rate is attributable to a profound decrease in MAR, indicating a decrease in the ability of individual osteoblasts to produce bone matrix. These findings were supported by the changes

Author Manuscript Author Manuscript Author Manuscript Author Manuscript

observed in osteoblast parameters. The Number of Osteoblasts (N.Ob/B.Pm) and Osteoblast Surface (Ob.S/B.Pm) were significantly decreased in male *Cthrc1* null mice. The same trend was seen in female mice, but did not reach statistical significance (25% lower N.Ob/B.Pm and 30% lower Ob.S/B.Pm), suggesting that in addition to a decrease in individual osteoblast activity there is also a decrease in the number of these cells. In agreement with Mineralizing Surface (MS) and MAR, Osteoid Surface (OS/BS) and Osteoid Thickness (O.Th) showed a significant decrease in both genders, confirming that *Cthrc1* null mice exhibit a defect in bone formation.

3.3. Effects of *Cthrc1* on mechanical properties of bone

Three-point bending tests and μCT were performed to compare the mechanical and architectural properties of bones from 8 week old male and female wildtype and *Cthrc1* null mice on the C57BL/6J background. μCT was performed on the mid-diaphysis of the femur to measure cortical architecture and mineral density. As shown in Table 2 and Fig. 2, female *Cthrc1* null mice had similar cortical architecture, and only a slight increase (not statistically significant) in cortical tissue mineral density relative to the wildtypes. In contrast, male *Cthrc1* null mice had worse cortical bone properties, including greater cortical porosity and lower femur length, cortical thickness, cortical tissue mineral density, cortical area, total area, cortical bone area fraction, and the maximum, minimum, and polar moments of inertia relative to the wildtype male mice. These μCT results predict that deletion of *Cthrc1* would have a negative effect on femoral biomechanical properties in male mice.

Three-point bending of the femoral diaphysis showed very little difference between the mechanical properties of the femurs from wildtype and *Cthrc1* null female mice, but, as predicted by the inferior bone morphology, there were significant deficits in *Cthrc1* null male mice. Specifically, male *Cthrc1* null mice had 29% lower maximum moment and 32% lower bending stiffness relative to wildtype mice (Table 2). While there was a decrease in bending stiffness in the *Cthrc1* null male mice, there was no difference in bending modulus, suggesting that the differences in biomechanical properties between the *Cthrc1* null and wildtype male mice are due to cortical bone architecture rather than the material properties of the bone. The bones of *Cthrc1* null male mice also required significantly less work (energy) to cause them to yield and fracture.

In summary, deletion of *Cthrc1* has minimal effects on cortical bone properties in female mice. In contrast, male *Cthrc1* null mice have shorter femurs, with reduced cross-sectional area and cortical morphology, leading to worse biomechanical properties compared to wildtype mice.

3.4. CTHRC1 does not affect osteogenic differentiation of BMSCs in vitro

To determine if CTHRC1 has a cell-autonomous effect on osteogenic differentiation of BMSCs, we isolated these cells from both wildtype and *Cthrc1* null mice and induced osteogenic differentiation by adding ascorbic acid and β-glycerophosphate. In contrast to previous reports (4,6), we found that BMSCs isolated from *Cthrc1* knockout mice can differentiate into osteoblasts as effectively as wildtype BMSCs as determined by Alizarin red and von Kossa staining (Fig. 3A–C). In addition, when we differentiate BMSCs derived

Author Manuscript Author Manuscript Author Manuscript Author Manuscript

from *Cthrc1* null mice in the presence of hCTHRC1 we found no difference between control-treated cells and hCTHRC1-treated cells with respect to osteogenic differentiation as determined by Alizarin red (Fig. 3D, E) and alkaline phosphatase staining (Fig. 3F, G). Proliferation of bone marrow stromal cells was not impacted by the presence or absence of CTHRC1 with similar numbers of colonies formed in both treatment groups (Fig. 3H). We also performed osteogenic differentiation in *Cthrc1* knockout BMSCs after transduction with an hCTHRC1 adenovirus or control adenovirus (Fig. 3I, J) and observed no effect on osteogenic differentiation. Therefore, our data indicate that for BMSCs growing *in vitro*, there is no cell-autonomous effect of CTHRC1 in regulating osteogenic differentiation.

3.5. CTHRC1 promotes osteogenic differentiation of calvarial osteoblasts *in vitro*

To determine whether the effects of CTHRC1 on osteogenic differentiation are cell type-dependent, we examined osteogenic differentiation also of calvarial osteoblasts derived from both *Cthrc1* null and wildtype mice. Although early osteogenic differentiation as assessed by alkaline phosphatase activity was similar among cultures (not shown), late stage differentiation markers were significantly reduced in *Cthrc1* null osteoblast cultures (Fig. 3K, L). We verified that osteoblast cultures were indeed expressing CTHRC1 by measuring CTHRC1 levels in the medium by ELISA while cells were in growth medium and differentiation medium (Fig. 3M, GM5, DM3). CTHRC1 was secreted into the medium by wildtype osteoblasts but not by *Cthrc1* null cells. These data indicate that CTHRC1 has cell-autonomous functions in calvarial osteoblasts.

3.6. Bone resorption is increased in *Cthrc1* null mice

We next examined bone resorption parameters, osteoclast number (N.Oc/B.Pm) and osteoclast surface (Oc.S/B.Pm), in wildtype and *Cthrc1* null mice. In contrast to previous reports, we observed that both parameters were significantly increased by approximately 41% and 47% in the male *Cthrc1* null mice, respectively (Table 1). In female mice, the osteoclast number in *Cthrc1* null mice is also significantly increased by approximately 36% when compared with wildtype mice (Table 1). Although the osteoclast surface was also increased in female *Cthrc1* null mice, it did not reach statistical significance (Table 1). Importantly, the Eroded Surface (ES/BS) was significantly increased in both genders (Table 1). These data clearly indicate that the lower trabecular bone mass observed in *Cthrc1* knockout mice is also the result of increased bone resorption activity, in addition to the decrease in bone formation. These data indicate that the lower trabecular bone mass observed in *Cthrc1* null mice is also the result of increased bone resorption activity, in addition to the decrease in bone formation.

3.7. CTHRC1 negatively regulates osteoclastogenesis

Based on our expression data (Fig. 1), CTHRC1 is expressed in osteoblasts and osteocytes. The significant upregulation of bone resorption in *Cthrc1* null mice suggests that osteoblast- and osteocyte-derived CTHRC1 may function as a key factor negatively regulating osteoclastogenic differentiation. To answer this question, we carried out *in vitro* osteoclastogenic differentiation assays using bone marrow-derived monocytes isolated from *Cthrc1* null mice. This approach avoided any potential effect of endogenous CTHRC1 produced by bone marrow cells. As shown in Fig. 4A and B, bone marrow monocytes are

Author Manuscript Author Manuscript Author Manuscript Author Manuscript

able to differentiate into multinucleated osteoclast in the presence of M-CSF and RANKL and this process is strongly inhibited in the presence of hCTHRC1 as demonstrated by fewer $TRAP^+$ osteoclasts (Fig. 4C). Of note, not only was the number of $TRAP^+$ osteoclasts decreased, the cells were also significantly smaller in size compared to control treated cells. As a measure of function, the bone resorption capacity of osteoclasts was also analyzed *in vitro* (Fig. 4D–F). The percentage of resorbed surface area was 63.8% ± 1.7% for osteoclast cultures supplemented with control-LacZ condition-medium, whereas in the presence of CTHRC1 condition-medium the resorbed surface area was significantly reduced to (46.9% ± 4.8%, Fig. 4F). Taken together, these data suggest that CTHRC1 derived from bone forming cells may serve as a key factor that negatively regulates osteoclast function. To support this notion even further, we isolated bone marrow monocytes from both wildtype and *Cthrc1* null mice, cultured them in osteoclast differentiation medium and found that inactivation of the *Cthrc1* gene had no effect on the osteoclast differentiation potential of bone marrow monocytes (Fig. 4G–I). This finding clearly indicated a role of extrinsic CTHRC1 in the osteoclast differentiation process of monocytes. We also determined by real-time RT-PCR the induction of genes associated with osteoclasts, such as *Trap*, *Ctsk*, *Rank*, c-*Fos*, and *Pparγ*. As shown in Fig. 5A, *Trap*, *Ctsk*, and *c-Fos* expression are significantly downregulated in the presence of CTHRC1 on days 4, 7, and 9 of differentiation. Although osteoblasts and osteocytes are considered major sources of *Opg*, which functions as a decoy receptor for *RANKL*, it was recently demonstrated that osteoclasts also express *Opg* (15). Interestingly, rather than an upregulation we observed a transient downregulation of *Opg* at day 2 of differentiation. Expression of *Rank* and *Pparγ* were not significantly affected by the presence of CTHRC1, suggesting that early stages of monocyte to macrophage differentiation are not influenced by CTHRC1. We also determined *c-Fos*, *Rankl*, *Nfatc1, Rank* and *Trap* gene expression within femurs from wildtype and *Cthrc1* null mice. As shown in Fig. 5B, *c-Fos, Nfatc1, Trap* and *Rankl* expression are significantly upregulated in *Cthrc1* null mice when compared with wildtype mice. *Rank* expression is similar among strains and *Opg* expression is downregulated in *Cthrc1* null mice. Taken together, these data indicate that CTHRC1 plays a pivotal role in inhibiting osteoclastogenic differentiation and bone resorption.

We determined M-CSF-stimulated early downstream signaling transduction by Western blotting. CTHRC1 had no effect on levels of p-ERK1/2, p-JNK1/2, or p-p38 (supplemental Fig. 1S). To gain additional insight into how CTHRC1 modulates osteoclastogenic differentiation, we utilized RAW264.7 cells, a macrophage cell line widely used for osteoclast formation. RANKL induced robust osteoclast formation in RAW264.7 cells in the presence of control-CM; however, the presence of hCTHRC1 almost completely abrogated osteoclast differentiation (Fig. 6A–C). This finding is consistent with effects of CTHRC1 seen in osteoclastogenic differentiation of primary bone marrow-derived monocytes (Fig. 4). To further verify that the inhibitory activity of osteoclastogenesis was indeed related to the presence of hCTHRC1 in the added conditioned-medium, we removed hCTHRC1 from the conditioned-medium with monoclonal antibodies followed by removal of the CTHRC1/antibody complexes by protein A chromatography. Depletion of the hCTHRC1-CM with antibodies completely abolished its inhibitory effect on osteoclastogenesis (Fig. 6D). The effectiveness of hCTHRC1 removal from the conditioned medium was further verified by

Author Manuscript Author Manuscript Author Manuscript Author Manuscript

ELISA (Fig. 6E), which showed that nearly all hCTHRC1 had been removed by this approach.

To determine at what stage CTHRC1 inhibits osteoclast differentiation, we started to add hCTHRC1 to osteoclastogenic cultures of RAW 264.7 cells at various stages of differentiation (Fig. 6B). CTHRC1 potently inhibited osteoclastogenesis when it was added within the first 2 days of initiation of differentiation, while exposure of differentiating cells to CTHRC1 at later stages did not inhibit osteoclastogenesis (Fig. 6A–C).

3.8. CTHRC1 negatively regulates RANKL-induced NFκB signaling activation

The data presented above establish that CTHRC1 blocks osteoclastogenesis rather than cell proliferation. RANKL plays a key role in the induction of osteoclast differentiation, whereas M-CSF promotes proliferation of osteoclast precursors as well as survival of osteoclasts and their precursors. Upon binding to its receptor RANK, RANKL rapidly activates the NFκB pathway by activating IKK, which phosphorylates inhibitory IκBα thereby targeting it for proteasomal degradation. Loss of IκBα then enables translocation of NFκB from the cytosol to the nucleus to activate transcription of the NFκB dependent target genes. Simultaneously, RANKL activates MAPKs, including ERK, p38, and JNK. Moreover, RANKL upregulates the osteoclastogenic transcription factor, NFATC1, and a number of osteoclast proteins, such as Cathepsin K (CTSK) and β3 integrin.

To test whether CTHRC1 inhibits osteoclastogenesis via modulation of RANKL signal transduction, we examined whether its downstream signaling activation is affected by CTHRC1. We observed that hCTHRC1 inhibits RANKL-induced phosphorylation and thus degradation of IκBα, resulting in reduced phosphorylation of NFκB (p65) at serine 536 (p-p65), which serves as a readout for NFκB signaling activation (Fig. 6F with quantification shown in Fig. 6H–I). Reduction in p-IκBα levels in the presence of hCTHRC1 (Fig. 6F, H) raises the possibility that CTHRC1 may be inhibiting IKKβ activity, thereby preventing phosphorylation of IκBα. We assessed potential effects of CTHRC1 on transcriptional activity of NFκB in RAW264.7 cells transfected with a NFκB luciferase reporter and stimulated with RANKL in the presence of hCTHRC1. As shown in Fig. 6J, hCTHRC1-CM completely blocked NFκB reporter activation in response to stimulation by RANKL. These data indicate that CTHRC1 inhibits RANKL-induced NFκB signaling activation by blocking phosphorylation and degradation of IκBα. Finding lower levels of IκBα in femurs of *Cthrc1* null mice (Fig. 6K) is consistent with increased NFκB signaling in the mutants. Expression of a constitutively active form of IKKβ (ca-IKKβ) completely reversed the inhibition of osteoclast differentiation by hCTHRC1, confirming that CTHRC1 inihibits NFκB signaling by inhibiting IKKβ activity (Fig. 6L, M).

CTHRC1 did not affect early ERK1/2 activation in response to stimulation by RANKL (Fig. 7A). However, levels of activated ERK1/2 (p-ERK1/2) were significantly lower at later stages of differentiation in the presence of hCTHRC1 as seen in Fig. 7A at 360 min and Fig. 7B with quantification shown in Fig. 7C and Fig. 7D, respectively. Consistent with inhibition of ERK1/2 activation by hCTHRC1 is the finding of reduced AP-1 luciferase reporter activity in RAW264.7 cells stimulated with RANKL in the presence of hCTHRC1

Author Manuscript Author Manuscript Author Manuscript Author Manuscript

(Fig. 7E). Western blotting also revealed elevated p-ERK1/2 levels in femur lysates from *Cthrc1* null mice compared to wildtypes (Fig. 7F).

3.9. Collagen antibody-induced arthritis is severely exacerbated in the absence of CTHRC1

The NFκB signaling pathway is an important pathway in inflammation. The inhibitory effects of CTHRC1 on NFκB signaling in osteoclasts and macrophage-like RAW264.7 cells prompted us to investigate the role of CTHRC1 in a collagen II antibody-induced arthritis model. We have recently documented abundant expression of CTHRC1 in activated fibroblast-like synoviocytes (FLS) forming the pannus (16). Cells eroding the bone surface show the highest levels of CTHRC1 expression (Fig. 8A). Scoring of arthritis in knee joints and ankle joints as well as quantification of pannus and eroded bone surface revealed vastly increased inflammation in *Cthrc1* null joints (Fig. 8D, F, G, H) compared to wildtypes (Fig. 8C, E, G, H).

4. Discussion

In the present study, we established that CTHRC1 is a key factor secreted by osteoblasts and some osteocytes (Fig. 1). We also demonstrated that CTHRC1 functions as a potent negative regulator of osteoclastogenesis by inhibiting RANKL-stimulated NFκB signaling activation and ERK1/2 phosphorylation. Bone formation *in vivo* was reduced in *Cthrc1* null mice. Although bone marrow stromal cells from *Cthrc1* null mutants can differentiate into osteoblasts as efficiently as wildtype cells *in vitro*, primary cultures of calvarial osteoblasts from newborn *Cthrc1* null mice differentiated less efficiently than their wildtype controls. These results indicate that cell-autonomous effects of CTHRC1 with regards to bone formation are cell type dependent.

Control of bone resorption is mediated by RANKL, which was expressed at higher levels in bones from *Cthrc1* null mice (Fig. 5B), suggesting that CTHRC1 may also affect bone mass by suppressing *Rankl* expression in addition to RANK signaling. A concomitant reduction in expression of the RANKL decoy receptor *Opg* (Fig. 5B) could further increase RANK signaling in *Cthrc1* null mice promoting bone resorption. Whether RANKL expression is altered also in other tissues remains to be determined. RANKL plays additional important roles in the maturation and activation of the immune system (17,18) with implications for therapies targeting rheumatoid arthritis. In the collagen II antibody-induced arthritis model we observed severely exacerbated arthritis in *Cthrc1* null mice with extensive inflammatory cell infiltration and pannus formation with extensive bone destruction. Only one of the wildtype mice showed arthritis in some joints by histology whereas all *Cthrc1* null mice developed arthritis, the majority with a maximal arthritis score (Fig. 8). These findings indicate that CTHRC1 has potent anti-inflammatory functions, suggestive of a broader role in immune responses.

Our studies also reveal that bones from males are more severely affect by the loss of *Cthrc1* than bones from females. This is supported not only by measurements of bone parameters but also by functional testing of bone strength (Table 1 and 2). Studies addressing the underlying mechanism for this gender discrepancy are beyond the scope of this study.

Author Manuscript Author Manuscript Author Manuscript Author Manuscript

Previous studies reported that CTHRC1 is a positive regulator of osteoblastic bone formation *in vivo* and *in vitro* (4,6). Using primary cultured bone marrow stromal cells *in vitro*, Kimura et al. reported that *Cthrc1* functions intrinsically as an autocrine protein to stimulate osteoblast proliferation and osteogenic differentiation (4). In contrast, Takeshita et al. reported that CTHRC1 acts as a coupling factor, expressed only by mature bone-resorbing osteoclasts, to stimulate osteoblastogenesis of calvarial osteoblastic cells *in vitro* (6). To reconcile these differing reports we generated panels of both rabbit and mouse monoclonal antibodies and validated them exhaustively for various applications, including immunohistochemistry on tissues from *Cthrc1* null mice as negative controls. Our data unequivocally demonstrate that CTHRC1 is not expressed by osteoclasts but rather by osteoblasts and some osteocytes (Fig. 1). Our data also show that during *in vitro* culture of bone marrow stromal cells *Cthrc1* gene expression gradually increases with progressive osteogenic differentiation (Fig. 1). This is consistent with our earlier reports of CTHRC1 production in activated stromal cells of remodeling muscle, heart, vasculature, as well as tumor stroma (2). In addition, we also recently demonstrated that progenitor cells derived from the stromal vascular fraction of adipose tissue express *Cthrc1* (5). Considering the association of CTHRC1 expression with tissue remodeling, it is perhaps not surprising that bone as a constantly remodeling tissue is the only tissue constitutively expressing CTHRC1 along with brain.

While we showed that CTHRC1 has cell type dependent effects on bone formation *in vitro*, an autocrine mechanism for stimulating bone formation *in vivo* may have limited impact considering that cortical bone formation is fairly normal in *Cthrc1* null mice, especially in females (Table 1 and 2). The more pronounced phenotype in trabecular bone of *Cthrc1* null mice is, however, consistent with a role of CTHRC1 in osteoclasts because per unit of bone volume more osteoclasts are present in trabecular bone than cortical bone.

Osteocyte cytoplasmic processes are on average 104 nm in diameter compared to the average 259 nm diameter of the canaliculi (19). Higher power views of CTHRC1 localization in bone reveal CTHRC1 in the thinner cytoplasmic processes close to the osteocyte cell body (Fig. 1D and E, arrows). The presence of CTHRC1 within the wider structure of the canaliculi (Fig. 1D and E, arrowheads) suggests that CTHRC1 is secreted from the osteocyte into the canalicular system, which is part of the interstitial space. The localization of CTHRC1 in the osteocyte canaliculi along with often prominent accumulations of CTHRC1 around intraosseal venules (Fig. 1F, arrows) would support the concept that osteocyte-derived CTHRC1 is contributing to circulating CTHRC1 levels observed in humans (2). The functions of circulating CTHRC1 are currently unknown, however, the association of elevated CTHRC1 levels in subjects known to have variant alleles of the melanocortin receptor MC1R suggests that the melanocortin system may be involved (2). CTHRC1 plasma levels in wildtype mice are typically below the detection limit of our assay (data not shown).

Takeshita et al. previously reported that global deletion of *Cthrc1* as well as osteoclast-specific deletion of *Cthrc1* both lead to lower bone mass due to decreased bone formation, while osteoblast-specific deletion of *Cthrc1 in vivo* does not affect bone mass (6). In their study, *CtsK-Cre* and *Osx-Cre* mice were crossed with mice carrying floxed *Cthrc1* alleles to

Author Manuscript Author Manuscript Author Manuscript Author Manuscript

generate osteoclast and osteoblast specific deletion of *Cthrc1*, respectively. Recent studies using *CtsK-Cre* mice revealed that Cre activity is not restricted to osteoclasts. Indeed, *CtsK-Cre* was shown to cause unexpected germline deletion of genes in mice (20). Additional concerns about the assumed osteoclast specificity of *CtsK-Cre* mediated recombination are also raised by a study demonstrating that *Ctsk* is expressed in mesenchymal progenitor cells, indicating that *Ctsk-Cre* mediated *Cthrc1* deletion will not be restricted to osteoclasts but instead could also target progenitor cells differentiating into bone-forming cells (7).

There are also potential issues with regards to the use of *Osx-Cre* mice for expressing Cre selectively in osteoblasts, osteocytes and hypertrophic chondrocytes, because a recent study reported *Osx* expression also in stromal cells, adipocytes, and perivascular cells of bone marrow (21). Although the relationship between marrow fat and bone is increasingly appreciated (22–24), the potential influence of stromal cells and perivascular cells on bone is still largely unknown. Given we demonstrated a role for CTHRC1 in adipogenic differentiation (5), the unintended recombination activity mediated by *Osx-Cre* may make interpretation of a postnatal bone phenotype more difficult than originally anticipated.

Our findings of increased bone resorption and arthritis reveal a novel aspect for the function of CTHRC1 in bone homeostasis (Fig. 4A–C). In cultures of bone marrow-derived monocytes from *Cthrc1* knockout mice, CTHRC1 exhibits strong inhibition of $TRAP^+$ multinucleated osteoclast formation together with significant downregulation of osteoclastogenic gene expression and pit-forming bone resorption activity (Fig. 4D–I). *Cthrc1* null cells can differentiate into osteoclasts as effectively as wildtype cells. These data support our *in vivo* findings and further support a role for CTHRC1 as a secretory protein from osteoblasts and osteocytes functioning as a key factor inhibiting osteoclastogenesis. In addition, CTHRC1 expression by activated fibroblast-like synoviocytes may have anti-inflammatory functions inhibiting arthritic joint destruction.

Osteoclast precursors originate from hematopoietic progenitor cells of the macrophage/monocyte lineage and the differentiation of these cells into bone-resorbing mature osteoclasts is a multistep process that involves cell proliferation, commitment, fusion, and activation (25,26). Our time-course experiments indicate that CTHRC1 strongly inhibits RANKL-induced osteoclast differentiation only when added at an early stage of differentiation (Fig. 6), indicating that CTHRC1 may affect signaling events in osteoclast precursors. M-CSF and RANKL are two major factors essential for osteoclast differentiation. Immunoblotting data indicate that CTHRC1 does not affect M-CSF-stimulated early downstream signal transduction, such as ERK1/2, JNK and p38 (Supplemental Fig. 1). With no effect of CTHRC1 on M-CSF-mediated cell proliferation, these findings indicate that CTHRC1 may exert its effect by modulating osteoclast differentiation. In support of this we found that CTHRC1 strongly inhibits RANKL-stimulated NFκB signaling activation by inhibiting phosphorylation and degradation of IκBα without affecting the activation of JNK and p38 (Supplemental Fig. 2). Although CTHRC1 did not affect early ERK1/2 activation after RANKL stimulation, it was associated with a significant reduction of ERK1/2 activation during later stages. ERK1/2 activation is known to be an essential step for transcriptional complex formation of AP-1 during

Author Manuscript Author Manuscript Author Manuscript Author Manuscript

RANKL-stimulated osteoclast formation; therefore, reduction of ERK1/2 activation by CTHRC1 may also contribute to its inhibition of osteoclast differentiation.

It has been reported that CTHRC1 can interact with Fzd and Ror2 to stabilize the WNT-receptor complex and activate the planar cell polarity pathway (27) through activation of Rac1 and RhoA. However, studies on bone from both *Wnt5a* and *Ror2* mutant mice indicate that both have increased bone mass (28). *In vitro* studies indicate that the Wnt5a-Ror2 signaling axis plays a positive role in regulating osteoclast formation by enhancing RANK expression in osteoclast precursors (28) via activation of JNK. On the other hand, it has been reported that Rac1 acting upstream of TAK1 to induce NFκB activation is required for the normal differentiation of osteoclast precursors (29,30), whereas RhoA was reported to inhibit osteoclast differentiation (31). Bone phenotypes of *Wnt5a* and *Ror2* mutant mice are the opposite of what we and others find in *Cthrc1* null mice, and furthermore, our *in vitro* data indicate that CTHRC1 has no effect on RANK expression and JNK activation (Fig. 5) (28). This suggests, that cell surface receptors mediating the biological effects of CTHRC1 have yet to be identified.

From a therapeutic point of view, as a secreted and circulating factor that inhibits osteoclastogenesis and immune responses, CTHRC1 may be a very attractive candidate to target conditions associated with low bone mass as well as arthritis.

Supplementary Material

Refer to Web version on PubMed Central for supplementary material.

Acknowledgements

This study was supported with funds from the Maine Medical Center Research Institute. The Mouse Transgenic and *In Vivo* Imaging Core facility (grant number P30GM103392, Phase III COBRE in Vascular Biology, R. Friesel, P.I.) and the Histopathology Core Facility (grant numbers P30GM103392 with R. Friesel, P.I. and P30GM103465 with D. Wojchowski, P.I.) were supported by the National Institute of General Medical Sciences. Sex hormone levels were measured by The University of Virginia Center for Research in Reproduction Ligand Assay and Analysis Core, which is supported by the Eunice Kennedy Shriver NICHD/NIH (NCTRI) Grant P50-HD28934. We would like to thank Dr. Anjana Rao for sharing the IKK-2S177E S181E construct (Addgene plasmid #11105). We would like to thank Phuong Le for assistance with the primary culture of osteoclasts. Y-RJ and JPS performed *in vivo* and *in vitro* studies and Y-RJ also prepared the manuscript. QW performed *in vitro* experiments, KN and RB provided histomorphometry data, MLB performed mechanical testing, CJR contributed to study design and data interpretation. VA designed and analyzed the arthritis data and contributed to manuscript writing. VL designed experiments, interpreted and generated data as well as reagents, and prepared the manuscript. Y-RJ and VL accept responsibility for integrity of the data analysis.

6. References

1. Pyagay P, Heroult M, Wang Q, Lehnert W, Belden J, Liaw L, Friesel RE, Lindner V 2005 Collagen triple helix repeat containing 1, a novel secreted protein in injured and diseased arteries, inhibits collagen expression and promotes cell migration. Circ Res 96(2):261–8. [PubMed: 15618538]
2. Duarte CW, Stohn JP, Wang Q, Emery IF, Prueser A, Lindner V 2014 Elevated plasma levels of the pituitary hormone cthrc1 in individuals with red hair but not in patients with solid tumors. PLoS One 9(6):e100449. [PubMed: 24945147]
3. Stohn JP, Perreault NG, Wang Q, Liaw L, Lindner V 2012 Cthrc1, a novel circulating hormone regulating metabolism. PLoS One 7(10):e47142. [PubMed: 23056600]

Author Manuscript Author Manuscript Author Manuscript Author Manuscript

4. Kimura H, Kwan KM, Zhang Z, Deng JM, Darnay BG, Behringer RR, Nakamura T, de Crombrugghe B, Akiyama H 2008 Cthrc1 is a positive regulator of osteoblastic bone formation. PLoS ONE 3(9):e3174. [PubMed: 18779865]
5. Stohn JP, Wang Q, Siviski ME, Kennedy K, Jin YR, Kacer D, DeMambro V, Liaw L, Vary CP, Rosen CJ, Prudovsky I, Lindner V 2015 Cthrc1 controls adipose tissue formation, body composition, and physical activity. Obesity (Silver Spring) 23(8):1633–1642. [PubMed: 26148471]
6. Takeshita S, Fumoto T, Matsuoka K, Park KA, Aburatani H, Kato S, Ito M, Ikeda K 2013 Osteoclast-secreted CTHRC1 in the coupling of bone resorption to formation. J Clin Invest 123(9): 3914–24. [PubMed: 23908115]
7. Yang W, Wang J, Moore DC, Liang H, Dooner M, Wu Q, Terek R, Chen Q, Ehrlich MG, Quesenberry PJ, Neel BG 2013 Ptpn11 deletion in a novel progenitor causes metachondromatosis by inducing hedgehog signalling. Nature 499(7459):491–5. [PubMed: 23863940]
8. Rowe GC, Vialou V, Sato K, Saito H, Yin M, Green TA, Lotinun S, Kveiborg M, Horne WC, Nestler EJ, Baron R 2012 Energy expenditure and bone formation share a common sensitivity to AP-1 transcription in the hypothalamus. J Bone Miner Res 27(8):1649–58. [PubMed: 22461201]
9. Zalli D, Neff L, Nagano K, Shin NY, Witke W, Gori F, Baron R 2016 The Actin-Binding Protein Cofilin and Its Interaction With Cortactin Are Required for Podosome Patterning in Osteoclasts and Bone Resorption In Vivo and In Vitro. J Bone Miner Res 31(9):1701–12. [PubMed: 27064822]
10. Bouxsein ML, Boyd SK, Christiansen BA, Guldberg RE, Jepsen KJ, Muller R 2010 Guidelines for assessment of bone microstructure in rodents using micro-computed tomography. J Bone Miner Res 25(7):1468–86. [PubMed: 20533309]
11. Dempster DW, Compston JE, Drezner MK, Glorieux FH, Kanis JA, Malluche H, Meunier PJ, Ott SM, Recker RR, Parfitt AM 2013 Standardized nomenclature, symbols, and units for bone histomorphometry: a 2012 update of the report of the ASBMR Histomorphometry Nomenclature Committee. J Bone Miner Res 28(1):2–17. [PubMed: 23197339]
12. Spatz JM, Ellman R, Cloutier AM, Louis L, van Vliet M, Suva LJ, Dwyer D, Stolina M, Ke HZ, Bouxsein ML 2013 Sclerostin antibody inhibits skeletal deterioration due to reduced mechanical loading. J Bone Miner Res 28(4):865–74. [PubMed: 23109229]
13. Kawai M, Green CB, Lecka-Czernik B, Douris N, Gilbert MR, Kojima S, Ackert-Bicknell C, Garg N, Horowitz MC, Adamo ML, Clemmons DR, Rosen CJ 2010 A circadian-regulated gene, Nocturnin, promotes adipogenesis by stimulating PPAR-gamma nuclear translocation. Proc Natl Acad Sci U S A 107(23):10508–13. [PubMed: 20498072]
14. DeMambro VE, Maile L, Wai C, Kawai M, Cascella T, Rosen CJ, Clemmons D 2012 Insulin-like growth factor-binding protein-2 is required for osteoclast differentiation. J Bone Miner Res 27(2): 390–400. [PubMed: 22006816]
15. Kang JH, Ko HM, Moon JS, Yoo HI, Jung JY, Kim MS, Koh JT, Kim WJ, Kim SH 2014 Osteoprotegerin expressed by osteoclasts: an autoregulator of osteoclastogenesis. J Dent Res 93(11):1116–23. [PubMed: 25256714]
16. Shekhani MT, Forde TS, Adilbayeva A, Ramez M, Myngbay A, Bexeitov Y, Lindner V, Adarichev VA 2016 Collagen triple helix repeat containing 1 is a new promigratory marker of arthritic pannus. Arthritis Res Ther 18:171. [PubMed: 27430622]
17. Kim D, Mebius RE, MacMicking JD, Jung S, Cupedo T, Castellanos Y, Rho J, Wong BR, Josien R, Kim N, Rennert PD, Choi Y 2000 Regulation of peripheral lymph node genesis by the tumor necrosis factor family member TRANCE. J Exp Med 192(10):1467–78. [PubMed: 11085748]
18. Kong YY, Yoshida H, Sarosi I, Tan HL, Timms E, Capparelli C, Morony S, Oliveira-dos-Santos AJ, Van G, Itie A, Khoo W, Wakeham A, Dunstan CR, Lacey DL, Mak TW, Boyle WJ, Penninger JM 1999 OPGL is a key regulator of osteoclastogenesis, lymphocyte development and lymph-node organogenesis. Nature 397(6717):315–23. [PubMed: 9950424]
19. You LD, Weinbaum S, Cowin SC, Schaffler MB 2004 Ultrastructure of the osteocyte process and its pericellular matrix. Anat Rec A Discov Mol Cell Evol Biol 278(2):505–13. [PubMed: 15164337]
20. Winkeler CL, Kladney RD, Maggi LB Jr, Weber JD 2012 Cathepsin K-Cre causes unexpected germline deletion of genes in mice. PLoS One 7(7):e42005. [PubMed: 22860046]

Author Manuscript Author Manuscript Author Manuscript Author Manuscript

21. Chen J, Shi Y, Regan J, Karuppaiah K, Ornitz DM, Long F 2014 Osx-Cre targets multiple cell types besides osteoblast lineage in postnatal mice. PLoS One 9(1):e85161. [PubMed: 24454809]
22. Fazeli PK, Horowitz MC, MacDougald OA, Scheller EL, Rodeheffer MS, Rosen CJ, Klibanski A 2013 Marrow fat and bone--new perspectives. J Clin Endocrinol Metab 98(3):935–45. [PubMed: 23393168]
23. Kawai M, Devlin MJ, Rosen CJ 2009 Fat targets for skeletal health. Nat Rev Rheumatol 5(7):365–72. [PubMed: 19468288]
24. Rosen CJ, Klibanski A 2009 Bone, fat, and body composition: evolving concepts in the pathogenesis of osteoporosis. Am J Med 122(5):409–14. [PubMed: 19375545]
25. Sims NA, Martin TJ 2014 Coupling the activities of bone formation and resorption: a multitude of signals within the basic multicellular unit. Bonekey Rep 3:481. [PubMed: 24466412]
26. Boyle WJ, Simonet WS, Lacey DL 2003 Osteoclast differentiation and activation. Nature 423(6937):337–42. [PubMed: 12748652]
27. Yamamoto S, Nishimura O, Misaki K, Nishita M, Minami Y, Yonemura S, Tarui H, Sasaki H 2008 Cthrc1 selectively activates the planar cell polarity pathway of Wnt signaling by stabilizing the Wnt-receptor complex. Dev Cell 15(1):23–36. [PubMed: 18606138]
28. Maeda K, Kobayashi Y, Udagawa N, Uehara S, Ishihara A, Mizoguchi T, Kikuchi Y, Takada I, Kato S, Kani S, Nishita M, Marumo K, Martin TJ, Minami Y, Takahashi N 2012 Wnt5a-Ror2 signaling between osteoblast-lineage cells and osteoclast precursors enhances osteoclastogenesis. Nat Med 18(3):405–12. [PubMed: 22344299]
29. Lee NK, Choi HK, Kim DK, Lee SY 2006 Rac1 GTPase regulates osteoclast differentiation through TRANCE-induced NF-kappa B activation. Mol Cell Biochem 281(1–2):55–61. [PubMed: 16328957]
30. Vives V, Laurin M, Cres G, Larrousse P, Morichaud Z, Noel D, Cote JF, Blangy A 2011 The Rac1 exchange factor Dock5 is essential for bone resorption by osteoclasts. J Bone Miner Res 26(5): 1099–110. [PubMed: 21542010]
31. Mizoguchi F, Murakami Y, Saito T, Miyasaka N, Kohsaka H 2013 miR-31 controls osteoclast formation and bone resorption by targeting RhoA. Arthritis Res Ther 15(5):R102. [PubMed: 24004633]

Author Manuscript Author Manuscript Author Manuscript Author Manuscript

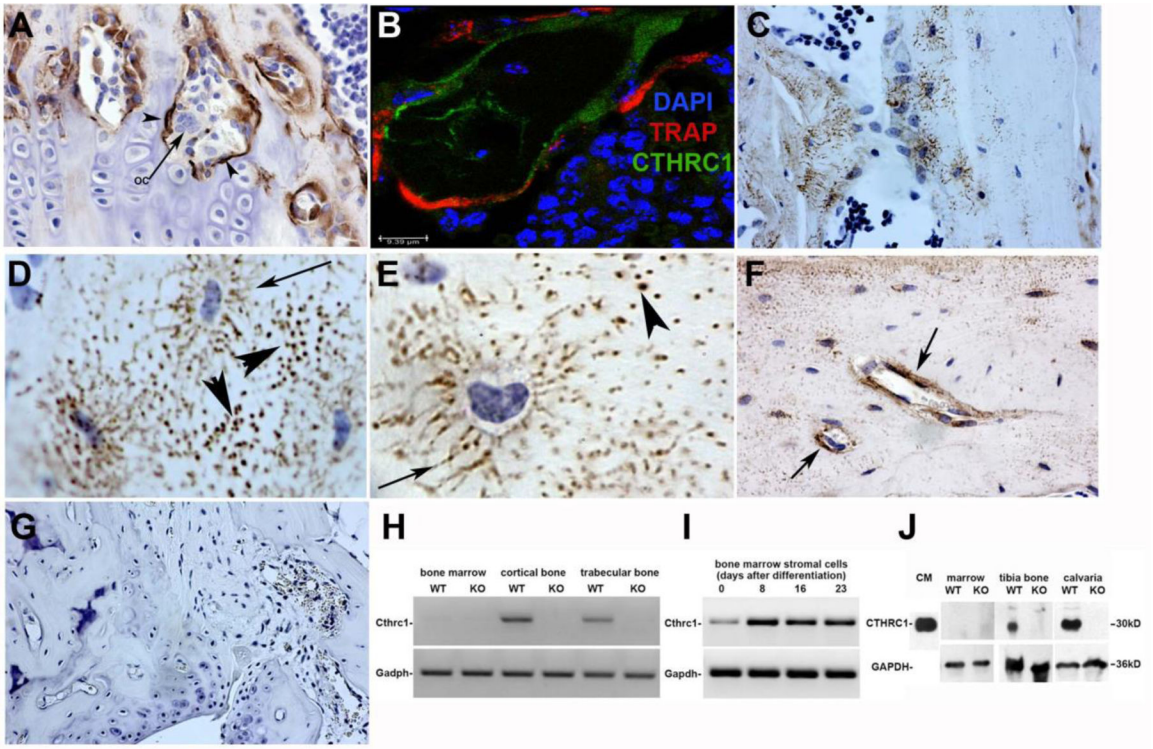

Figure 1. CTHRC1 is expressed in bone by osteoblasts and osteocytes, not osteoclasts.

(A) Monoclonal anti-CTHRC1 antibody reveals CTHRC1 in osteoblasts (arrowheads) and osteocytes of trabecular and cortical bone in wildtype mice, whereas multinucleated osteoclasts (arrows) do not express CTHRC1. (B) Confocal imaging of TRAP (red) and CTHRC1 (green) immunohistochemistry of a bone trabeculum shows no overlap, demonstrating that CTHRC1 is not expressed in cells expressing the osteoclast marker TRAP (nuclear stain with DAPI). (C) Note the distinct localization of CTHRC1 in canaliculi of some osteocytes. (D, E) CTHRC1 is found in the thin cytoplasmic processes of osteocytes (arrow). Immunoreactive CTHRC1 appears to be present in the wider canaliculi (arrows) indicating secretion of CTHRC1 into the interstitial fluid. (F) Prominent accumulation of CTHRC1 is frequently seen around venules (arrows). (G) CTHRC1 is not detectable in trabecular bone of *Cthrc1* knockout mice demonstrating antibody specificity. (H) *Cthrc1* expression was analyzed by RT-PCR using mRNA isolated from bone fractions of metaphysis and proximal epiphysis (trabecular bone), diaphysis (cortical bone), as well as bone marrow, which does not express *Cthrc1*. (I) *Cthrc1* mRNA expression was analyzed in primary bone marrow-derived mesenchymal stromal cells during osteogenic differentiation. (J) Western blot analysis of CTHRC1 from femur and marrow lysates obtained from wildtype and *Cthrc1* null mice shows CTHRC1 in bone but not the marrow fraction.

Author Manuscript Author Manuscript Author Manuscript Author Manuscript

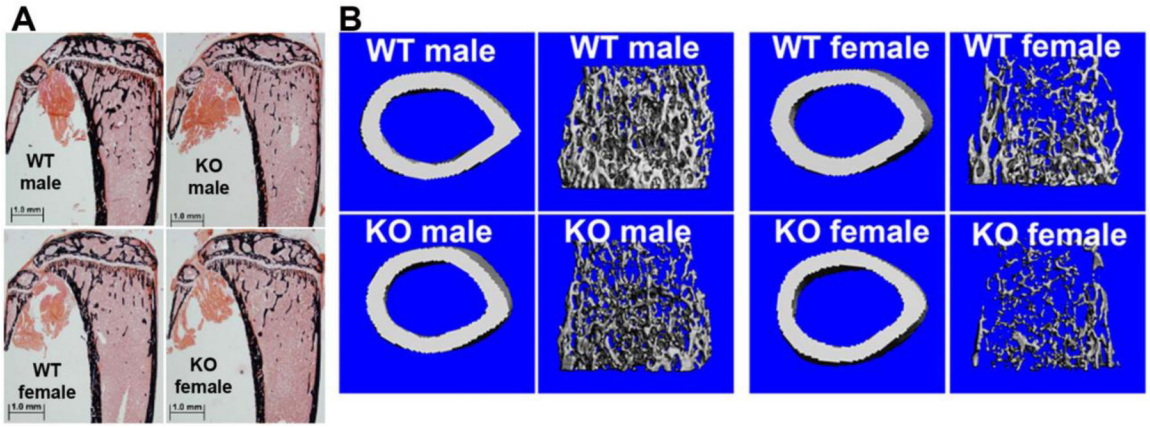

Figure 2. Bone formation and bone strength are reduced in *Cthrc1* null mice.

(A) von Kossa staining of proximal tibia sections of *Cthrc1* null and wildtype mice is shown. (B) Representative micro-CT images of cortical and trabecular bone show decreased trabecular bone in *Cthrc1* knockout mice.

Author Manuscript Author Manuscript Author Manuscript Author Manuscript

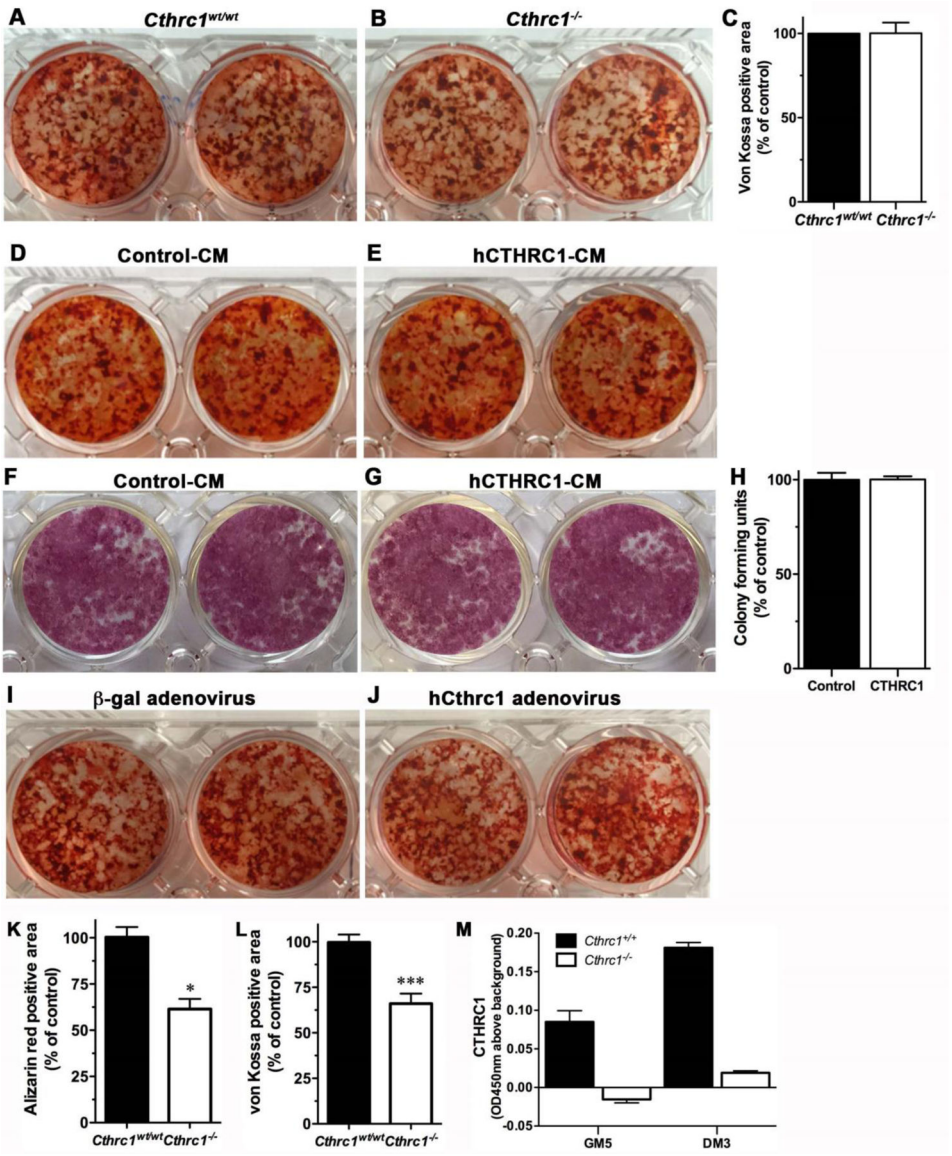

Figure 3. CTHRC1 does not affect osteogenic differentiation of bone marrow derived stromal cells or bone formation *in vitro*.

Alizarin red staining shows similar mineral content in bone marrow-derived stromal cells isolated from (A) wildtype or (B) *Cthrc1* null mice after induction of osteogenic differentiation. (C) Bone marrow stromal cell cultures from wildtype and *Cthrc1*$^{-/-}$ mice form similar amounts of bone *in vitro* as determined by von Kossa staining. (D, E) Alizarin red staining (D, E) and alkaline phosphatase activity staining (F, G) show that differentiation of bone marrow-derived stromal cells isolated from *Cthrc1*$^{-/-}$ mice in the presence of control conditioned-medium (Control-CM) or hCTHRC1 (hCTHRC1-CM) is similar. von Kossa staining showed similar results (not shown). (H) Bone marrow stromal cell proliferation was unaffected by the presence or absence of CTHRC1 with similar numbers of colonies formed. (I, J) Following transduction with control adenovirus (b-gal) or hCTHRC1 adenovirus bone marrow-derived stromal cells isolated from *Cthrc1* null mice revealed similar osteogenic differentiation potential. (K, L) Calvarial osteoblast cell cultures

Author Manuscript Author Manuscript Author Manuscript Author Manuscript

from *Cthrc1* null mice showed reduced bone formation as determined by decreased Alizarin red and von Kossa staining. (M) CTHRC1 was secreted into the medium by wildtype osteoblast cultures as determined by ELISA (GM5- day 5 in growth medium, DM3- day 3 in differentiation medium). Differentiation was performed over a 20-day period for all experiments. *$p<0.05$, ***$p<0.005$.

Author Manuscript Author Manuscript Author Manuscript Author Manuscript

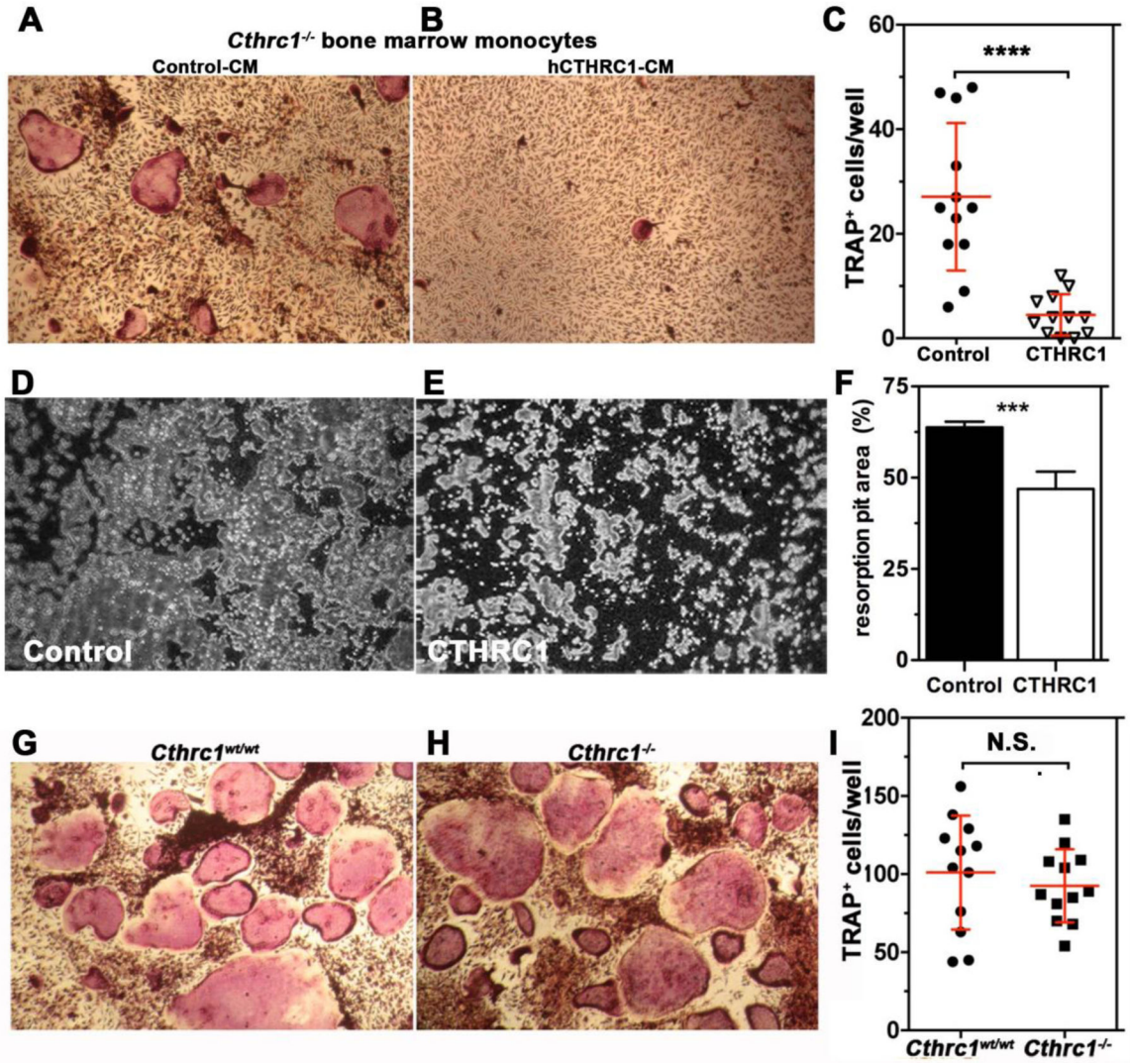

Figure 4. Cthrc1 negatively regulates osteoclastogenesis *in vivo* and *in vitro*.

(A-C) Histochemistry for TRAP was performed on differentiated osteoclasts of bone marrow-derived monocytes derived from *Cthrc1* null mice following 9 days of differentiation in the presence of control conditioned medium (CM, Control-CM) or hCTHRC1-containing CM. (C) TRAP positive multinucleated (>3 nuclei) osteoclasts were counted in each well. Data represent means±SD and are averages of ≥3 experiments. (D-F) *In vitro* bone resorption assays performed with osteoclast cultures from wildtype mice showed reduced bone resorption (pits in grey) in the presence of CTHRC1 (E) compared to control treated cells (D) with quantification shown in (F). Unresorbed bone matrix appears black. (G, H) Osteoclasts derived from bone marrow monocytes isolated from wildtype and *Cthrc1* knockout mice differentiated similarly as determined by TRAP histochemistry performed after 7 days of differentiation. (I) Number of TRAP positive multinucleated osteoclasts (>3 nuclei) were similar for both genotypes. Data represent means±SEM. ***p<0.005, **** p<0.001, N.S. = not significant.

Author Manuscript Author Manuscript Author Manuscript Author Manuscript

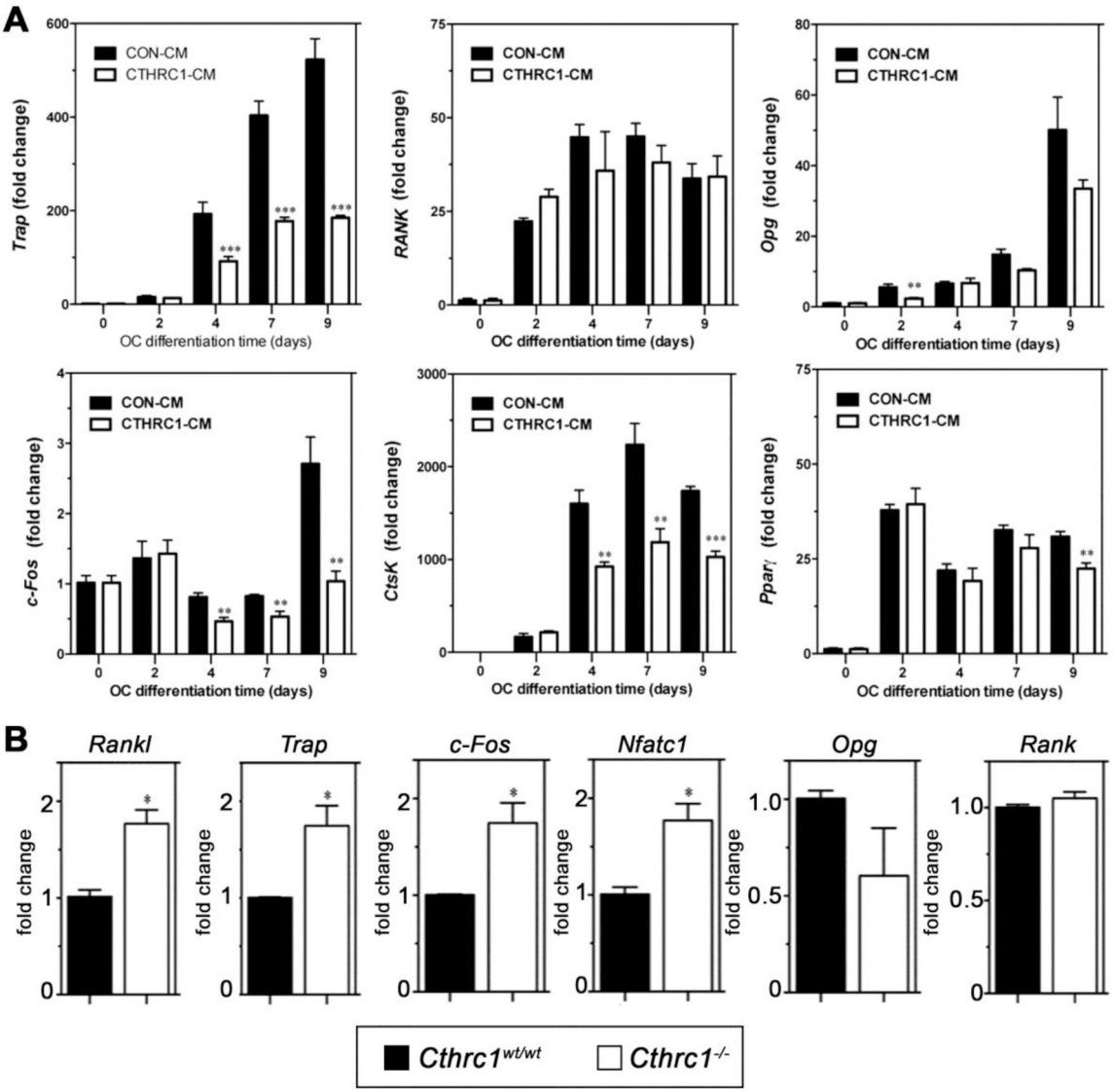

Figure 5. Cthrc1 negatively regulates osteoclastogenic marker gene expression *in vivo* and *in vitro*.

(A) Bone marrow-derived monocytes from *Cthrc1* knockout mice were cultured in osteoclastogenic differentiation medium containing control-CM (CON-CM) or hCTHRC1-CM for the indicated time periods. mRNA expression of *Trap*, *c-Fos*, *Rank*, *Opg*, *CtsK*, and *Pparγ* was analyzed by real-time RT-PCR. B) mRNA expression of *Trap*, *c-Fos*, *Rankl*, *Opg*, *Nfatc1*, and *Rank* in femurs of 3 month old wildtype and *Cthrc1* knockout mice was analyzed by real-time RT-PCR. Data represent means±SEM with ** indicating p<0.01 and *** indicating p<0.005.

Author Manuscript Author Manuscript Author Manuscript Author Manuscript

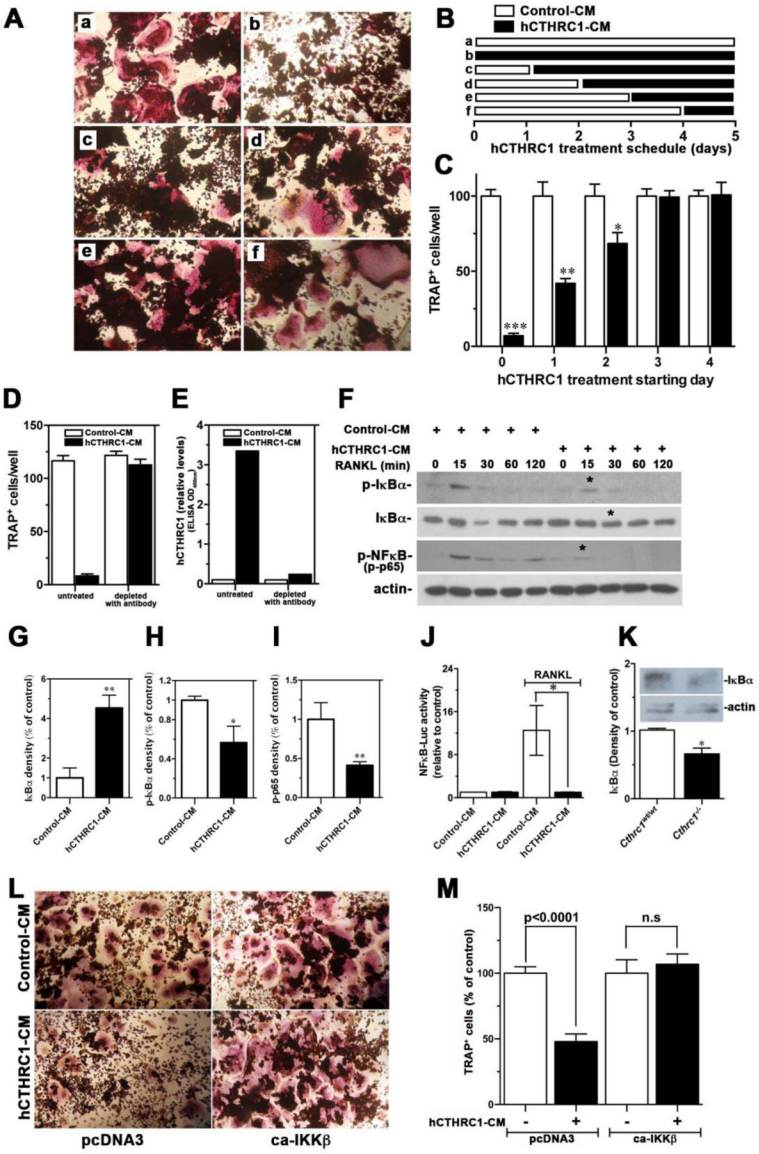

Figure 6. Effects of CTHRC1 on RANKL-induced osteoclastogenic differentiation and intracellular signaling transduction in RAW264.7 cells.

(A-C) RAW264.7 cells were differentiated with RANKL for 5 days and the time-dependent presence of hCTHRC1 to inhibit osteoclast differentiation was assessed. TRAP-positive multinucleated cells were quantified. Data represent means±SEM of ≥3 experiments with hCTHRC1-CM versus control-CM treated cells. (D) Osteoclast differentiation of RAW264.7 cells in the presence of hCTHRC1 (hCTHRC1-CM) is inhibited. Depleting hCTHRC1-CM with anti-CTHRC1 monoclonal antibodies abolishes this effect, demonstrating specificity. (E) Effectiveness of hCTHRC1-CM depletion was verified by measuring hCTHRC1 levels before and after depletion using an established ELISA. (F) RAW264.7 cells were stimulated with RANKL for the indicated length of time in the presence of hCTHRC1 or control medium. Western blotting of cell lysates shows reduced activation of NFκB (p-NFκB), reduced degradation of IκBα and reduced phosphorylation of IκBα (p-IκBα in the presence of hCTHRC1 (asterisks). (G-H) Quantification of immunoblot data marked with *

Author Manuscript Author Manuscript Author Manuscript Author Manuscript

in (F) are shown. (J) hCTHRC1 inhibits RANKL-induced NFκB-dependent luciferase reporter activity. (K) Western blot analysis of IκBα levels in femur lysates from wildtype and *Cthrc1* null mice shows significantly reduced levels in the mutants. (L, M) RAW264.7 cells treated with control-CM or hCTHRC1-CM were transfected with control vector (pcDNA3) or a vector expressing a constitutively active form of IKKβ (ca-IKKβ), which reversed inhibition of osteoclast differentiation by hCTHRC1. All data represent means ±SEM of replicates ≥3 with * = $p<0.05$, ** = $p<0.01$, and *** = $p<0.005$.

Author Manuscript Author Manuscript Author Manuscript Author Manuscript

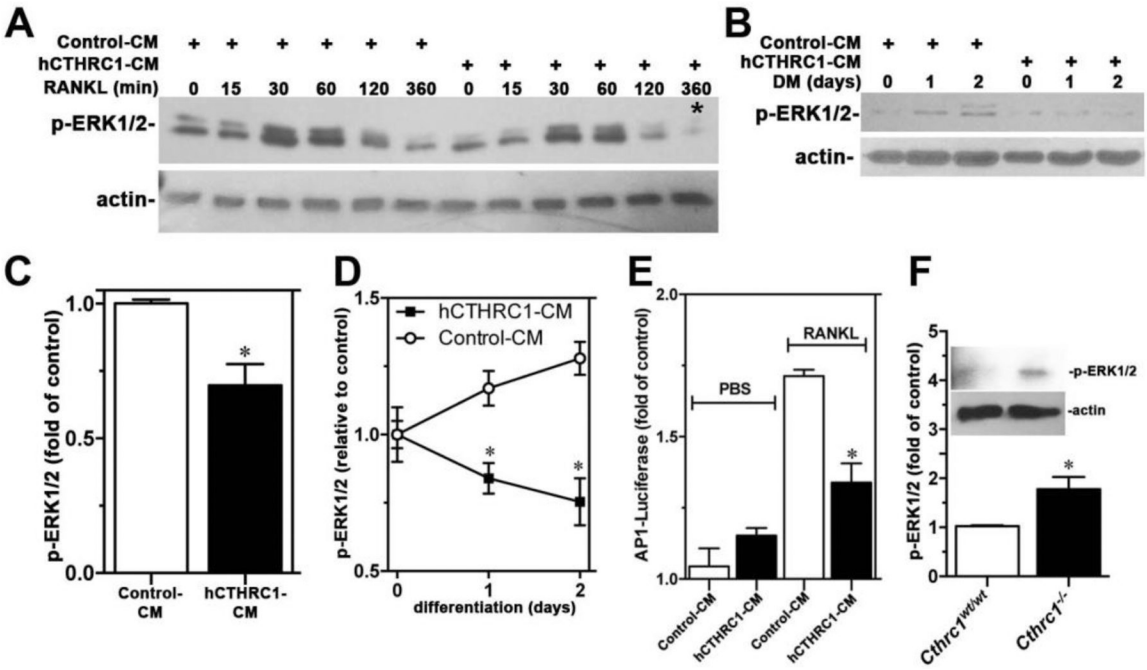

Figure 7.

(A) An immunoblot analysis of a time course of ERK1/2 activation (p-ERK1/2) in RAW264.7 cells stimulated with RANKL in the presence of control-CM or hCTHRC1-CM is shown. The corresponding quantification of the signal marked with * is shown in (C). In (B) p-ERK1/2 levels in RAW264.7 cells growing in differentiation medium (DM) for up to 2 days are shown with corresponding quantification shown in (D). (E) hCTHRC1 inhibits RANKL-induced AP-1 luciferase reporter activity in RAW264.7 cells transfected with the AP-1 promoter reporter plasmid. (F) Western blot analysis of p-ERK1/2 level in femur lysates from wildtype and *Cthrc1* null mice. All data represent means±SEM of replicates ≥3 with * = $p<0.05$.

Author Manuscript Author Manuscript Author Manuscript Author Manuscript

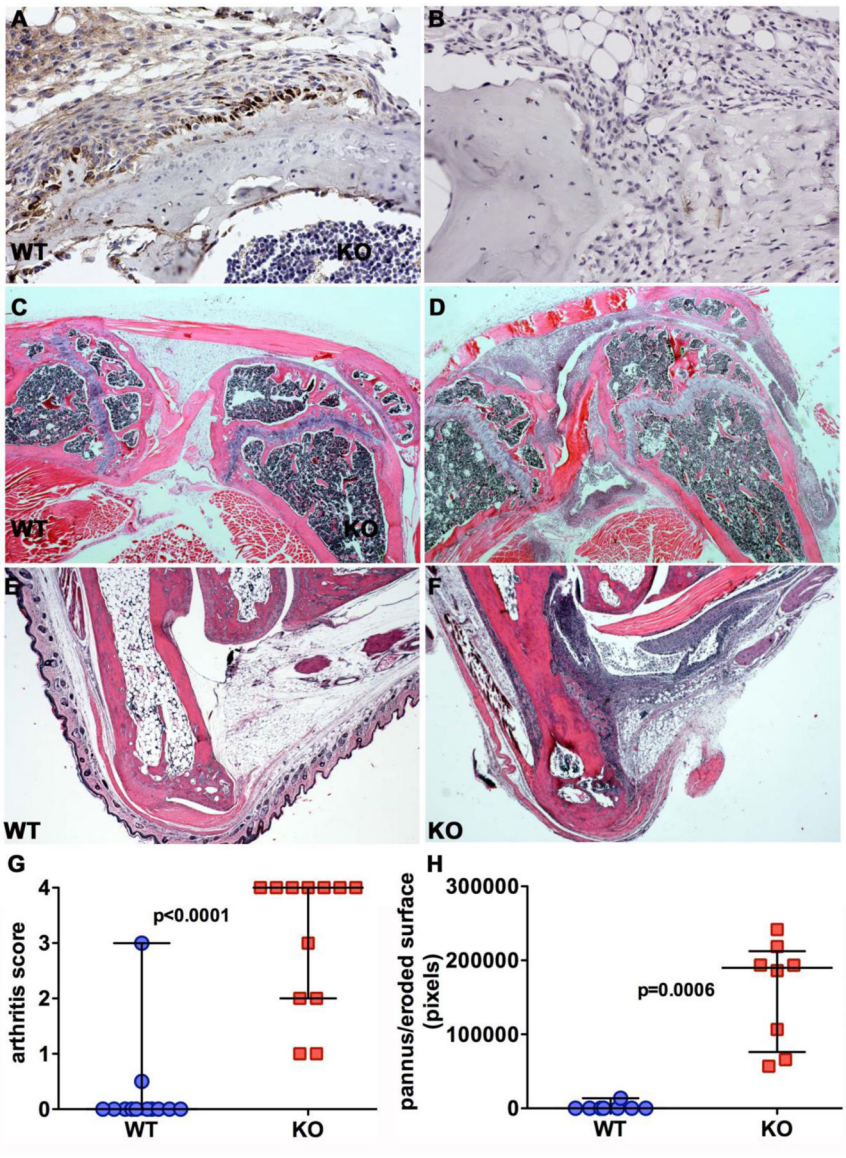

Figure 8. Loss of *Cthrc1* exacerbates arthritis in a collagen antibody-induced arthritis model.

(A) CTHRC1 immunohistochemistry was performed on sections of knee joints from wildtype (WT) and (B) *Cthrc1* null mice 21 days after collagen antibody injection. Fibroblast-like activated synoviocytes of the pannus show prominent expression of CTHRC1, most pronounced in cells near the eroded bone surface. Absence of immunoreactive CTHRC1 in *Cthrc1* null bones (B) demonstrates specificity of the staining. Representative images show hematoxylin-eosin stained sections of knee (C, D) and ankle joints (E, F) from *Cthrc1* null and wildtype mice with extensive inflammatory cell infiltrates, large pannus formation and bone erosion in D and F. (G) The degree of inflammation in knee joints and ankle joints was scored in a blinded fashion on a scale from 0 to 4 (“no” - “max” inflammation). *Cthrc1* null mice showed significantly larger pannus when compared to wildtype mice (Mann-Whitney U test). Each symbol represents a separately scored

histological section at 150x magnification. Horizontal lines are medians with interquartile range.

Author Manuscript Author Manuscript Author Manuscript Author Manuscript

Author Manuscript

Author Manuscript

Author Manuscript

Author Manuscript

Table 1:

Histomorphometry was performed on tibiae of 8 week old *Cthrc1* null mice (*Cthrc1*$^{tm1\,Vli}$) and corresponding wildtype mice (WT) on the C57BL/6J background. Data are means ± SD.

	Males		**Females**	
	WT (n=6)	**Cthrc1^{tm1Vli} (n=6)**	**WT (n=6)**	**Cthrc1^{tm1Vli} (n=6)**
BV/TV (%)	13.0±3.91	8.60±1.72*	10.3±3.94	5.60±0.91*
Tb.Th (μm)	33.3±5.33	24.9±3.03**	33.6±5.52	27.3±3.33*
Tb.N (/mm)	3.85±0.58	3.45±0.43	3.00±0.71	2.06±0.32*
Tb.Sp (μm)	232±43.6	269±36.7	317±89.9	470±79.2*
MAR (μm/day)	1.91±0.30	1.39±0.30*	1.98±0.24	1.32±0.12**
MS/BS (%)	27.9±5.20	27.6±1.70	25.6±3.10	21.8±3.60
BFR/BV (%/year)	1157±154.6	1088±215.6	1155±137.0	761.4±193.3**
BFR/BS ($\mu m^3/\mu m^2$/year)	193±38.7	140±30.3*	185±27.	106±24.9**
N.Ob/B.Pm (/mm)	8.40±1.68	5.82±0.86**	12.5±3.83	9.40±4.20
Ob.S/B.Pm (%)	13.3±3.15	9.10±1.69*	20.9±6.51	14.4±6.23
OS/BS (%)	10.4±3.96	3.57±1.47**	8.86±2.68	4.45±1.28**
O.Th (μm)	6.49±0.73	5.52±0.73*	6.49±0.98	5.01±0.97*
N.Oc/B.Pm (/mm)	1.62±0.22	2.28±0.38**	2.52±0.56	3.42±0.75*
Oc.S/B.Pm (%)	4.52±1.11	6.65±1.32*	7.39±1.83	9.82±2.47
ES/BS (%)	2.29±0.68	3.82±0.86**	2.76±0.87	5.04±1.39**

*denotes statistically significant with $p<0.05$;

**denotes statistically significant with $p<0.01$.

Author Manuscript Author Manuscript Author Manuscript Author Manuscript

Table 2:

Results for three-point bending and μCT analyses performed on femurs from 8 week old *Cthrc1* null mice (*Cthrc1*$^{tm1\,Vli}$) and corresponding wildtype mice (WT) on the C57BL/6J background are shown. Data are means ± SD.

	Males		Females	
	WT (n=6)	**Cthrc1^{tm1Vli} (n=6)**	**WT (n=6)**	**Cthrc1^{tm1Vli} (n=6)**
Three-point bending data				
Max. Moment (N-mm)	30.15±4.49	21.38±3.40**	23.29±1.87	20.30±3.12
Bending stiffness (N-mm^2)	838±142	566±159**	744±131	641±115
Estimated Modulus (GPa)	6.43±1.25	6.19±1.42	8.33±1.58	7.71±0.64
Mid-diaphysis μCT data				
Femur length (mm)	14.55±0.20	13.75±0.20**	13.84±0.61	13.62±0.40
Ct.Th (mm)	0.161±0.011	0.123±0.006**	0.132±0.012	0.121±0.013
Ct.TMD (mgHA/cm^3)	1030±8	1014±6**	1012±18	1040±14
Ct.Ar (mm^2)	0.774±0.114	0.555±0.037**	0.574±0.042	0.518±0.061
Ma.Ar (mm^2)	1.201±0.125	1.208±0.058	1.103±0.069	1.125±0.023
Tt.Ar (mm^2)	1.975±0.238	1.763±0.088*	1.677±0.059	1.644±0.066
Ct.Ar/Tt.Ar (%)	39.10±1.29	31.48±1.07**	34.26±2.70	31.47±2.55
Ct. Porosity (%)	0.442±0.166	0.613±0.088*	0.518±0.138	0.500±0.034
pMOI (mm^4)	0.424±0.111	0.279±0.030**	0.267±0.020	0.239±0.033
I_{max} (mm^4)	0.289±0.078	0.187±0.021**	0.177±0.014	0.156±0.020
I_{min} (mm^4)	0.135±0.034	0.092±0.010**	0.090±0.009	0.083±0.013

*Denotes statistically significant with $p<0.05$;

**denotes statistically significant with $p<0.01$.